Pyroxene-garnet equilibration during cooling in the mantle

Douglas Smith, Barbara R. Barron

Department of Geological Sciences, University of Texas, Austin, Texas 78713, U.S.A.

Abstract

Compositional gradients at pyroxene-garnet contacts have been analyzed by electron microprobe to evaluate calculated temperatures and pressures and the kinetics of equilibration of pyroxene in mantle xenoliths. Samples are (1) garnet peridotite xenoliths from African kimberlites, (2) websterites containing exsolved garnet from the Sullivan Buttes Latite of central Arizona, and (3) pyrope megacrysts with enstatite and diopside inclusions from ultramafic diatremes on the Colorado Plateau. Orthopyroxene in group 1, with calculated $T \approx 800$ °C, is homogeneous in Fe, Mg, and Ca but has gradients of Al_2O_3 (0.98–0.85 wt%) over ≈ 500 μm in one rock and of Cr in two; a Cr gradient in one garnet is steeper than the gradients in pyroxene. Pyroxene-garnet T in groups 2 and 3 are 600–700 °C, and olivine-garnet T in group 3 are <600 °C. Orthopyroxene is zoned in Al and Mg in groups 2 and 3 but has steep gradients of Ca and Fe only in group 3. Diopside in group 3 is zoned in Al, Cr, Na, and Mg.

Fe-Mg equilibration appears to take place over distances >100 μm during cooling to $T \approx 700$ °C. Temperatures calculated for pyroxene-garnet pairs using analyses made within several micrometers of mutual contacts typically are not more than 70 °C lower than those based on analyzed points separated by 200 μm. Under appropriate conditions, equilibration of Al is maintained during cooling to $T \approx 800$ °C and of Cr to a somewhat higher T. Al gradients in orthopyroxene are largely fixed during cooling from ≈ 800 to 650 °C. The radial Al gradient in an orthopyroxene of group 3 has been simulated numerically. Activation energies for Al diffusion are ≥ 400 kJ/mol in the simulations that best match the measured gradient. A minimum diffusion coefficient for Al, based on an estimated slow limit for cooling rate, is $\approx 6 \times 10^{-25}$ m²/s at ≈ 800 °C. Qualitative comparisons of cation mobilities in garnet and pyroxene have also been made from gradients at contacts. The mobility of Cr appears to be less in garnet than pyroxene at $T \geq 800$ °C. Ca and Fe mobilities appear comparable in the two minerals at 600–800 °C.

Introduction

Diffusion rates in pyroxenes are not well known despite their importance for interpretations of calculated temperatures, pressures, and ages of rocks. Experiments and natural assemblages have been interpreted to indicate that diffusion in pyroxene may be slower than in garnet, and diffusion of Al in pyroxene may be particularly slow (Freer et al., 1982; Sautter et al., 1988a, 1988b; Sautter and Harte, 1988). If pyroxenes do not continuously equilibrate in the mantle, then temperatures and pressures calculated for some xenoliths may represent fossil or unrealized conditions (Harte and Freer, 1982; Fraser and Lawless, 1978). Isotopic disequilibrium between pyroxenes and associated minerals also may result from cooling at sufficiently fast rates or low temperatures (e.g., Hofmann and Hart, 1978; Sneeringer et al., 1984; Stosch et al., 1986) as demonstrated by Jagoutz (1988), who found distinct Nd isotope ratios in different generations of garnet within one mantle eclogite.

Few experimental measurements of diffusion in pyroxene have been made, and these measurements were at temperatures higher than those in much of the lithosphere. For instance, the mobility of Al in pyroxene has been measured only in diopside at and above 1100 °C (Seitz, 1973; Sautter et al., 1988a, 1988b). Furthermore, diffusivities in synthetic compounds may not be appropriate for minerals in the mantle: Sneeringer et al. (1984) measured Sr diffusion rates in natural and synthetic diopside at 1200–1300 °C and found rates 2 orders of magnitude faster in the natural samples. O vacancies (Huebner and Voigt, 1988) and hydroxide (Skogby and Rossman, 1989; Skogby et al., 1990) are present in variable concentrations in natural pyroxenes and may affect diffusion rates. Proton activity and pressure may have dramatic effects upon the diffusion rate of Al in silicates, as indicated by studies of Al-Si ordering in feldspars (Goldsmith, 1990; Graham and Elphick, 1990). Because the experimental data are sparse and of uncertain applicability, laboratory measurements do not yet provide strong constraints on the problem of pyroxene equilibration during mantle cooling.

Temperatures and pressures calculated from pyroxene

compositions provide information about equilibration rates. Harte and Freer (1982) noted that few temperatures calculated for mantle xenoliths are below 800 °C and that temperatures calculated from pyroxene equilibria mostly are above 900 °C, although the upper part of the cratonic mantle is expected to be at lower temperature. They suggested that mineral equilibria were frozen long before eruption in many low-T xenoliths. In contrast, Frost and Chacko (1989, p. 437) have proposed for crustal rocks that ". . . the closure temperature for two-pyroxene reequilibration even in a relatively rapidly cooled contact metamorphic environment lies below 700 °C." Equilibration rates may be faster in crustal environments than in the mantle. Anovitz (1989), however, has argued that prograde zonation of Al in pyroxene may be preserved in some crustal granulites. Pyroxenes can equilibrate by recrystallization as well as by intracrystalline diffusion, so low calculated temperatures do not necessarily document the effectiveness of diffusion.

The role of diffusion in reequilibration during cooling can be documented when compositional gradients formed by interaction between minerals are present at grain boundaries. Lasaga (1983) discussed the interplay of diffusion rates, cooling rates, and exchange reactions in forming such gradients. Sautter and Harte (1988, 1990) carefully analyzed diffusion gradients in clinopyroxene adjacent to exsolved garnet in an eclogite xenolith from the Roberts Victor kimberlite; they concluded that Fe-Mg equilibration between clinopyroxene and garnet lamellae ceased when a temperature of about 1000 °C was reached during cooling and that Al diffusion in clinopyroxene became ineffective at a temperature above 1000 °C. Based on their experiments at 1180 °C, Sautter et al. (1988a) also suggested that Al diffusion in diopside might be negligible at temperatures below 1000 °C.

In this study, compositional gradients at garnet-pyroxene contacts in three groups of xenoliths have been analyzed to investigate the role of diffusion in maintaining equilibrium in rocks that are cooled within the mantle and then quenched on eruption. Xenoliths were selected with calculated temperatures that are low, in the range 500–900 °C for most geothermometers. One group of samples consists of garnet peridotite xenoliths from kimberlites on the Kaapvaal craton in southern Africa. The second group consists of websterites with exsolved garnet from the xenolith localities in the Sullivan Buttes Latite in west central Arizona. The third group is pyrope megacrysts from the serpentinized ultramafic diatremes of the Navajo field on the Colorado Plateau; enstatite and diopside are included in some of the pyrope grains.

SAMPLES AND TECHNIQUES

Analytical techniques

Most analyses were made with a JEOL733 electron probe using beam currents of 40–50 nA and maximum count times of 40–60 s; counting was terminated if a precision in the range 0.1–0.3 relative percent (1σ) was attained. The limiting precisions were based solely on counting statistics of the single peak and associated background. Representative values of these limits for precision (as percent coefficient of variation, 1σ) in a typical clinopyroxene analysis are SiO_2, 0.3%; TiO_2, 4%; Al_2O_3, 0.5%; Cr_2O_3, 0.9%; FeO, 1.6%; MgO, 0.3%; CaO, 0.5%; Na_2O, 1%. Positions of analyses were recorded on photographs, and analyses were repeated to investigate the possibility that instrumental drift was responsible for apparent compositional zonation.

Garnet peridotite xenoliths from African kimberlites

Two peridotite xenoliths from southern Africa were selected. Rock J34 is a harzburgite from the varied suite of inclusions in the Jagersfontein kimberlite (Hops et al., 1989; Harte and Gurney, 1982; Winterburn et al., 1990). The rock is one of three low-temperature Jagersfontein xenoliths described by Smith and Wilson (1985); they documented that garnet in the rock appeared homogeneous. The rock contains amphibole like that described as metasomatic by Winterburn et al. (1990). Equant crystals of orthopyroxene and garnet in contact have been analyzed in additional detail. Rock PHN 4803 is a harzburgite xenolith from Lekkerfontein. Garnet occurs in "necklace" textures at the margins of orthopyroxene grains in the rock (Fig. 1A), and analyses were made to search for gradients associated with grain boundary exsolution of the garnet. All olivine in this rock has been altered to serpentine. Alteration zones, typically at least a few tens of micrometers thick, separate garnet and orthopyroxene in each rock, and so true contact compositions could not be measured.

Websterites with exsolved garnet, Chino Valley, Arizona

Gradients have been analyzed in two websterite xenoliths from the Sullivan Buttes Latite of west central Arizona (Arculus and Smith, 1979; Schulze and Helmstaedt, 1979; Arculus et al., 1988). Exsolution lamellae of orthopyroxene, garnet, and very rare clinopyroxene are intergrown in websterite Pr35 (Fig. 1B). Arculus and Smith (1979) used broad-beam analysis to reconstruct the average composition of these intergrowths; the composition is that of magmatic orthopyroxene with 6.7 wt% Al_2O_3. Because of garnet exsolution and other reactions, the orthopyroxene now has 1.5–0.5 wt% Al_2O_3. The second websterite, Prs90q, contains garnet at boundaries of mosaic grains of orthopyroxene and diopside; although all garnets appear to have formed by grain-boundary exsolution, some garnets are equant and euhedral, others are anhedral and inclusion rich, and some are skeletal. Orthopyroxene in Prs90q preserves an unusually large range of Al_2O_3, from 7 wt% distant from garnet to as little as 1.1 wt% by garnet contacts.

These xenoliths had a complex history that included cooling after an igneous origin, local recrystallization and formation of amphibole, and reheating by the host latites. The garnet-pyroxene intergrowths discussed here appear unaffected by late-stage amphibole formation and heating.
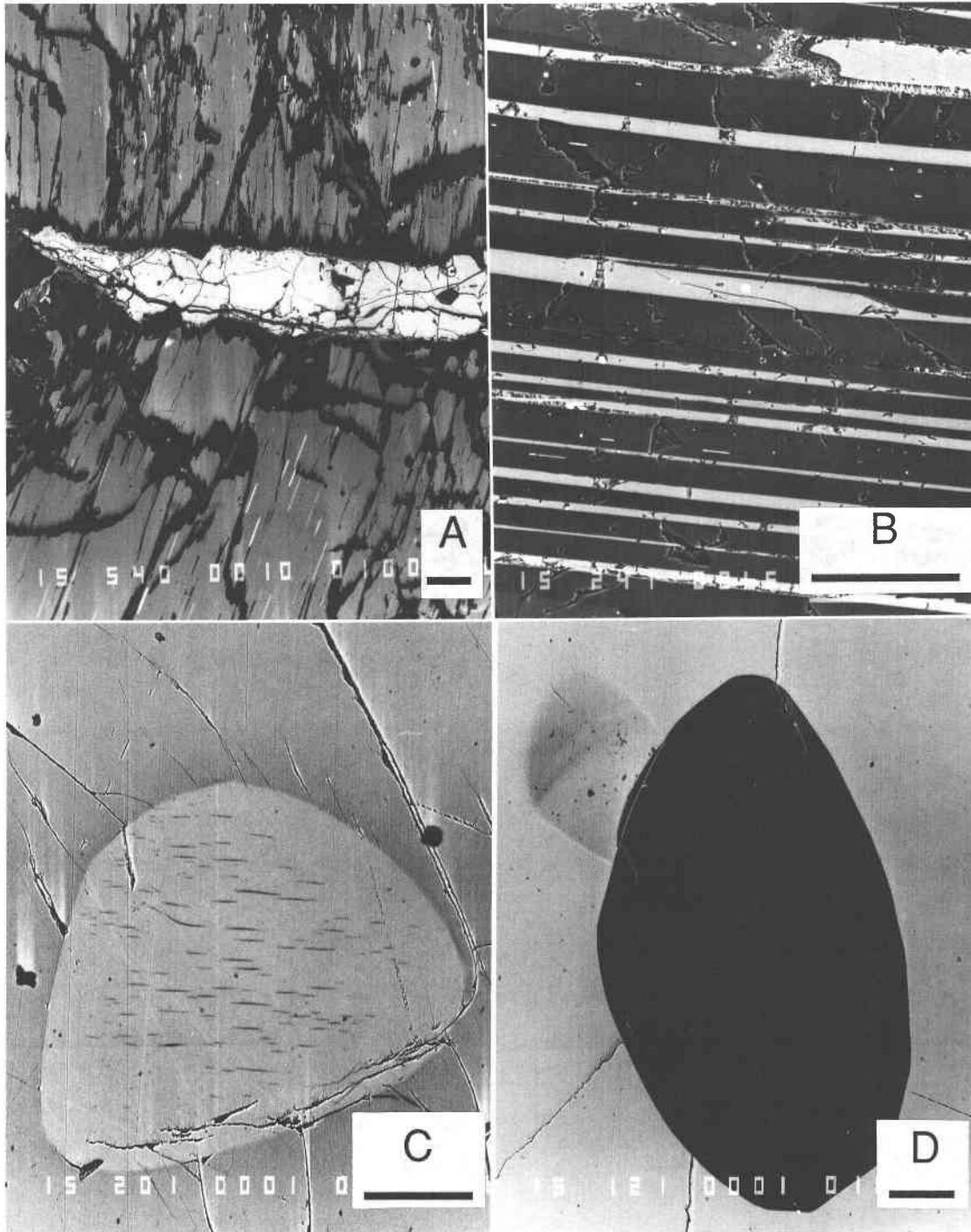
Fig. 1. Backscattered electron images of some of the analyzed garnet-pyroxene contacts. Scale bars are 100 μm. (A) Garnet (bright) separating two orthopyroxene grains (dark) in PHN 4803, Lekkerfontein, South Africa. (B) Orthopyroxene (dark) and garnet (bright) lamellae in websterite Pr35, Sullivan Buttes latite, Arizona. One of the bright lamellae is clinopyroxene. (C) Diopside inclusion in garnet 10, GR1, Garnet Ridge, Arizona. Dark lamellae are enstatite. (D) Enstatite inclusion in garnet 1, GR1, Garnet Ridge, Arizona.

TABLE 1. Calculated temperatures and pressures and selected compositional parameters

	Gar 1, GR1 Garnet Ridge, Navajo field, Arizona	Gar 10, GR1 Garnet Ridge, Navajo field, Arizona	Pr35 Sullivan Buttes Latite, Arizona	Prs90q Sullivan Buttes Latite, Arizona	J34 Jagersfontein kimberlite, South Africa	PHN 4803 Lekkerfontein kimberlite, South Africa
Opx-gar T, P (1)	650, 1.8	—	610, 1.7 to 710, 2.1	640, 1.7	800, 2.9	820, 2.8
Opx-gar T at P (2)	760 at 2.0	—	720 to 810 at 2.0	750 at 2.0	930 at 3.0	940 at 3.0
Cpx-gar T at P (3)	—	660 at 2.0	610 to 650 at 2.0	630 at 2.0	830 at 3.0	780 at 3.0
Cpx-gar T at P (4)	—	750 at 2.0	700 to 740 at 2.0	720 at 2.0	920 at 3.0	870 at 3.0
Cpx-opx T (5)	—	—	770	830	820	880
Cpx-opx-gar T, P (6)	—	—	700, 2.1	800, 2.4	800, 2.9	880, 3.2
Ol-gar T at P (7)	520 to 570 at 2.0	570 at 2.0	—	—	780 at 3.0	—
Wt% Al_2O_3 in opx	1.1–1.7	—	0.75–1.4	1.1–6.9	0.75	0.86–0.98
Fe/(Fe + Mg) opx	0.06	—	0.2	0.13	0.07	0.07
Ca gradients in opx?	yes	—	no	no	no	no
Cr gradients in opx?	yes	—	Data inadequate	yes	yes	yes

Note: T in °C and P in GPa. References are (1) Harley (1984a, 1984b), (2) Lee and Ganguly (1988), (3) Krogh (1988), (4) Ellis and Green (1979), (5) Wells (1977), (6) Brey and Kohler (1990), (7) O'Neill and Wood (1979).

Pyroxene inclusions in pyrope megacrysts, Colorado Plateau

Olivine, pyroxene, and less common phases are included in pyrope megacrysts from serpentine-rich diatremes of the Navajo field (McGetchin and Silver, 1970; Hunter and Smith, 1981; Smith, 1987). Hunter and Smith (1981) calculated that olivine-garnet pairs recorded cooling to 500–700 °C, and they noted that higher temperatures calculated from pyroxene-garnet pairs might be a result of disequilibrium during cooling. Griffin et al. (1989) analyzed some of the olivine-garnet pairs by proton microprobe and found Ni partitioning consistent with the low Fe-Mg temperatures. Fe-Mg gradients in pyrope about the homogeneous olivine inclusions were analyzed by Wilson and Smith (1984) and Smith and Wilson (1985), and they used numerical simulations to investigate what cooling rates could produce these gradients.

Pyroxene-garnet contacts in these megacrysts are ideally suited for electron probe analysis of diffusion gradients produced during cooling. Reheating by the transporting medium was at most minor because no magmatic component has been identified in the serpentine-rich breccias that contain the garnets (Roden, 1981). Contacts are free from alteration (Figs. 1C and 1D), and no evidence of recrystallization was observed. Because the pyroxenes are enclosed in garnet, they were isolated from reactions with all other phases except for sparse exsolved rutile at inclusion contacts. In particular, the compositional gradients record diffusion in the absence of any volatile phase. The megacryst source was not anhydrous, however, as some garnets include chlorite and other hydrous minerals (McGetchin and Silver, 1970; Hunter and Smith, 1981; Smith, 1987), and some have a structural hydrous component (Aines and Rossman, 1984). Skogby et al. (1990) found 0.073 wt% OH in a diopside megacryst from this locality.

Two garnets from the Garnet Ridge diatreme were ground and polished repeatedly in order to study sections through the centers of inclusions. A rounded diopside grain about 400×600 μm in maximum cross section and much smaller diopside and olivine grains were included in one garnet about 3 mm in diameter (garnet 10, GR1; analysis 258C of Hunter and Smith, 1981). The diopside inclusion contains exsolved lenses of enstatite, at most several micrometers thick, concentrated in the interior of the grain (Fig. 1C). The host garnet, like other pyrope megacrysts from these diatremes, is nearly homogeneous; garnet near the crystal rim is slightly richer in Cr and Fe than in the interior, and compositional gradients also are present within a few tens of micrometers of the diopside inclusion. An ovoid enstatite inclusion, about 450×800 μm in maximum cross section, and three smaller olivine inclusions were analyzed in the second garnet (garnet 1, GR1; analysis 356 of Hunter and Smith, 1981) (Fig. 1D). Single rutile grains were observed at contacts of both the enstatite and the diopside inclusions.

T and P calculated from the analyzed assemblages

Temperatures and pressures (Table 1) have been calculated with a variety of algorithms using compositions obtained near mineral contacts (Appendix Table 1). Accuracies of the calculated values are difficult to judge, in part because of the Fe^{3+} problem (e.g., Luth et al., 1990) and in part because compositional zonation documents disequilibrium during cooling. Moreover, the temperatures are below those of calibration experiments, and even accuracies of higher temperatures are in dispute (e.g., Carswell and Gibb, 1987; Finnerty and Boyd, 1987; Finnerty, 1989; Brey and Kohler, 1990).

Brey and Kohler (1990) evaluated thermobarometers for peridotite assemblages used in experiments. For orthopyroxene-garnet pairs held at 900 °C and 3–5 GPa, the thermobarometer of Harley (1984a) yielded values from about 900 to 1000 °C, whereas that of Lee and Ganguly (1988) yielded temperatures above 1000 °C. For clinopyroxene-garnet pairs, the thermobarometer of Krogh (1988) yielded temperatures in the range 890–950 °C,
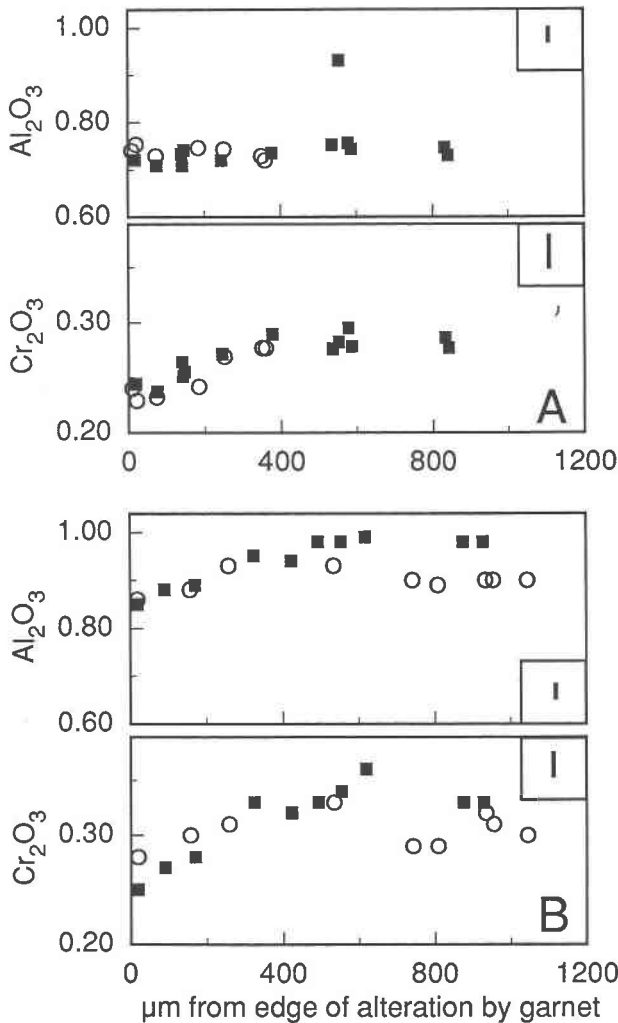
Fig. 2. Wt% Cr_2O_3 and Al_2O_3 in orthopyroxene on traverses from contacts with garnet. Data for two orthopyroxene crystals are shown for each rock. In this and in subsequent figures, the bars in each frame are 4 sd in length, as calculated solely from counting statistics of the peak and background measured at a representative point. (A) J34, Jagersfontein, South Africa. (B) PHN 4803, Lekkerfontein, South Africa (grains in Fig. 1A).

Fig. 3. Wt% Al_2O_3 and CaO in orthopyroxene on traverses perpendicular to garnet lamellae, extending into the interiors of three orthopyroxene lamellae in rock Pr35 (Fig. 1B), a websterite xenolith from the Sullivan Buttes Latite, Arizona.

of Ellis and Green (1979), as are results based on Krogh (1988).

Using the preferred calibrations of Harley (1984a) and Krogh (1988), temperatures recorded near garnet-pyroxene contacts are 780–830 °C in the two African xenoliths and 610–660 °C in the four Arizona xenoliths (Table 1). The temperature difference of 100–200 °C between these two ranges is better established than the absolute values. The 500–600 °C values calculated for olivine-garnet pairs from Arizona may record cooling to temperatures lower than those registered by pyroxene-garnet, as suggested by Hunter and Smith (1981). Brey and Kohler (1990) found no systematic bias between temperatures of their experiments and olivine-garnet temperatures based on O'Neill and Wood (1979).

COMPOSITIONAL GRADIENTS AT GARNET-PYROXENE CONTACTS

Two traverses at garnet-orthopyroxene contacts were analyzed in each of the African harzburgites; suitable garnet-diopside contacts were not found. Ca, Fe, Mg, Na, Si, and Ti appeared homogeneous in orthopyroxene, but Cr is zoned to slightly lower values within about 400 μm of garnet in each rock. Al is similarly zoned in PHN 4803 but is homogeneous in J34 (Figs. 2A and 2B). Garnet in J34 appears homogeneous (Smith and Wilson, 1985, their Fig. 6). In rock PHN 4803, a garnet selvage between two orthopyroxene grains (Fig. 1A) is homogeneous with about 3.6 wt% Cr_2O_3 except for a rim preserved at one orthopyroxene contact; garnet in this rim is sharply zoned to 2.6 wt% Cr_2O_3 over a distance of about 30 μm, with corresponding changes in other oxides.

whereas that of Ellis and Green (1979) yielded higher, more discrepant values. Judging from these comparisons, the Krogh (1988) and Harley (1984a) temperatures in Table 1 are the most accurate for equilibration of Fe-Mg near pyroxene-garnet contacts, although the values may be too high. The recent garnet-clinopyroxene thermometer of Pattison and Newton (1989) was not used for these assemblages because the authors advise against use for garnets more magnesian than their calibration samples. Garnets in four of our samples are too magnesian, and all are less calcic than the calibrated range. Pattison and Newton (1989) did note that temperatures based on their algorithm commonly are lower than values based on that
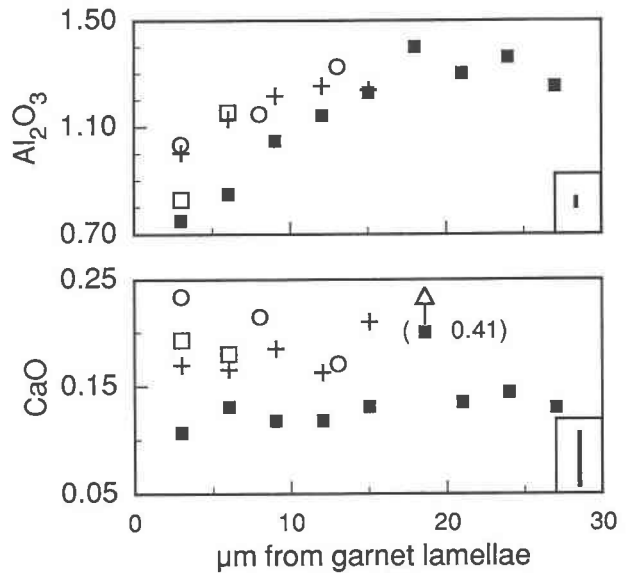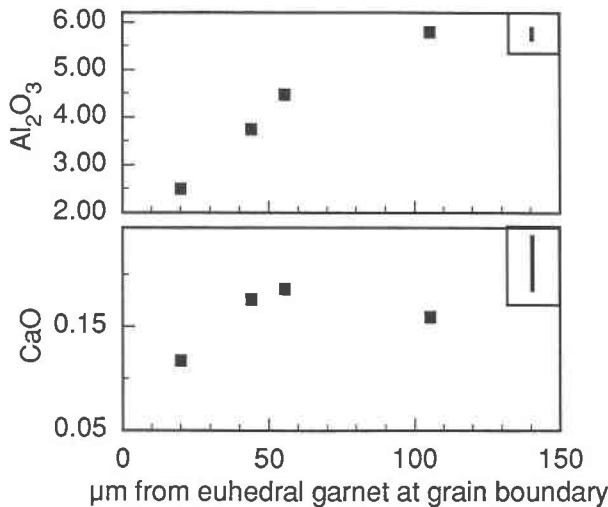
Fig. 4. Wt% Al₂O₃ and CaO in a mosaic grain of orthopyroxene in rock Prs90q, along a traverse line extending inward from a garnet crystal at the grain edge. The websterite xenolith is from the Sullivan Buttes Latite, Arizona.

Al is the most systematically zoned element in orthopyroxene lamellae in websterite Pr35. Al₂O₃ is 0.75 to 1.1 wt% within 5 μm of garnet but about 1.4 wt% at 15–20 μm distance (Fig. 3). Orthopyroxene contains as little as 0.53 wt% Al₂O₃ near amphibole and in recrystallized mosaic grains, but these low values may have been caused by amphibole formation. CaO appears homogeneous in individual lamellae, although a readily resolvable range (0.12–0.22 wt%) was found between lamellae (Fig. 3); the few higher CaO outliers are attributed to unresolved lamellae of clinopyroxene. Compositional zonation was not observed in garnet lamellae, and Ca/(Ca + Fe + Mg) was in the range 0.127–0.146 for all garnet, including mosaic grains. One mosaic grain is smoothly zoned from core ($Ca_{14.4}Fe_{40.2}Mg_{45.4}$) to rim ($Ca_{13.2}Fe_{43.0}Mg_{43.8}$) over a distance of 170 μm.

Mosaic grains of pyroxene in websterite Prs90q preserve high-temperature alumina contents in grain interiors not near garnet (7 wt% Al₂O₃ in orthopyroxene, 8.5 wt% in clinopyroxene). Orthopyroxene is zoned to about 1.1 wt% Al₂O₃ at garnet contacts (Figs. 4 and 5) and clinopyroxene to about 5 wt%. Cr is zoned sympathetically with Al in orthopyroxene, and Mg is zoned inversely. The relative homogeneity of Ca in orthopyroxene contrasts with the zonation of Al (Figs. 4 and 5). Garnet adjacent to orthopyroxene is zoned to higher Fe and Cr but lower Ca.

The enstatite inclusion in Navajo pyrope is zoned in Ca and Fe as well as in the trivalent cations Al and Cr (Figs. 6 and 7); the crystal has a relatively uniform interior about 200 μm wide, with pronounced gradients only within about 100 μm of the enclosing garnet. Ti gradients in enstatite and garnet extend to low values at the contact.
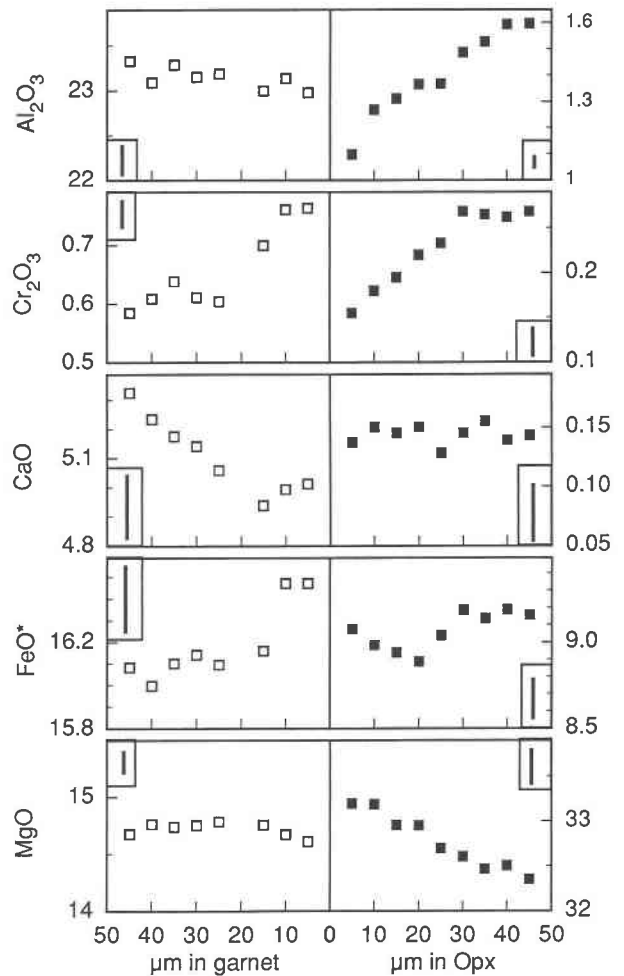

Fig. 5. Wt% oxides at 5-μm intervals across a garnet-orthopyroxene contact in rock Prs90q (not the same grain as in Fig. 4). "FeO*" in all figures represents Fe$_{tot}$ as FeO.

Garnet is zoned to higher Fe/Mg at the contact but appears homogeneous in Ca (Fig. 7).

Zonation of the diopside inclusion is most pronounced for Al, Cr, Na, and Mg (Fig. 8). The deviant points at about 120 μm from the contact are due to one of the enstatite exsolution lamellae; these lamellae were not thick enough for reproducible analysis. The garnet is zoned in Ca, Ti, Al, and Cr at the diopside contact, and the Cr gradients extend for similar distances ($\approx$30 μm) in each mineral.

DISCUSSION

Interpretations of gradients

The gradients preserved in these pyroxenes near garnet contacts formed as a consequence of reactions during cooling. Exchange reactions occurred, and garnet also grew as a result of the temperature dependence of the solubility of Al-Tschermak's component in pyroxene. Sautter and
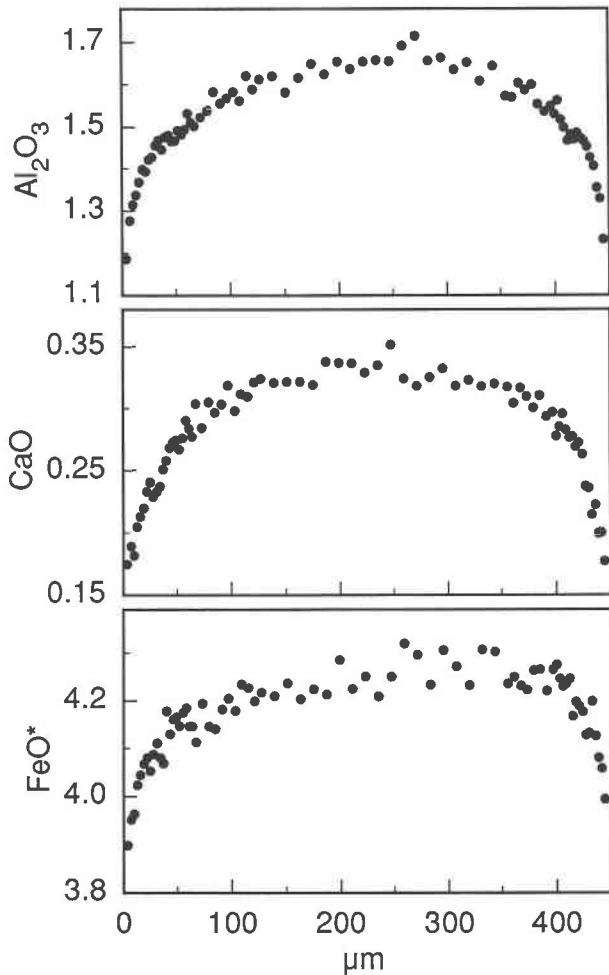
Fig. 6. Wt% Al₂O₃, FeO*, and CaO across the shorter radius of an enstatite inclusion in garnet (garnet 1, GR1, Garnet Ridge, Arizona—shown in Fig. 1D). Data for these three oxides only were collected with an older three-spectrometer, manual instrument.

Harte (1988) have described these reactions in more detail. The preserved gradients are evidence that the pyroxene did not recrystallize, and so these gradients and the calculated temperatures can be used to evaluate the kinetics of pyroxene equilibration by diffusion in the cooling mantle. Diffusion rates in pyroxene are dependent upon crystallographic direction (Sneeringer et al., 1984; Sautter and Harte, 1988), but crystallographic orientations of the traverse paths have not been evaluated, as the dependences on direction are expected to be minor compared to other uncertainties.

In the harzburgite orthopyroxenes, all elements except Cr and Al appear to have equilibrated by diffusion over distances of at least 400 μm during cooling (Fig. 2). The gradient in the thin rim of garnet in PHN 4803 (3.5–2.6 wt% Cr₂O₃ over a distance of 30 μm) is much steeper than in adjacent orthopyroxene (0.35–0.25 wt% over 500 μm). Homogeneity of J34 garnet contrasts with the slight
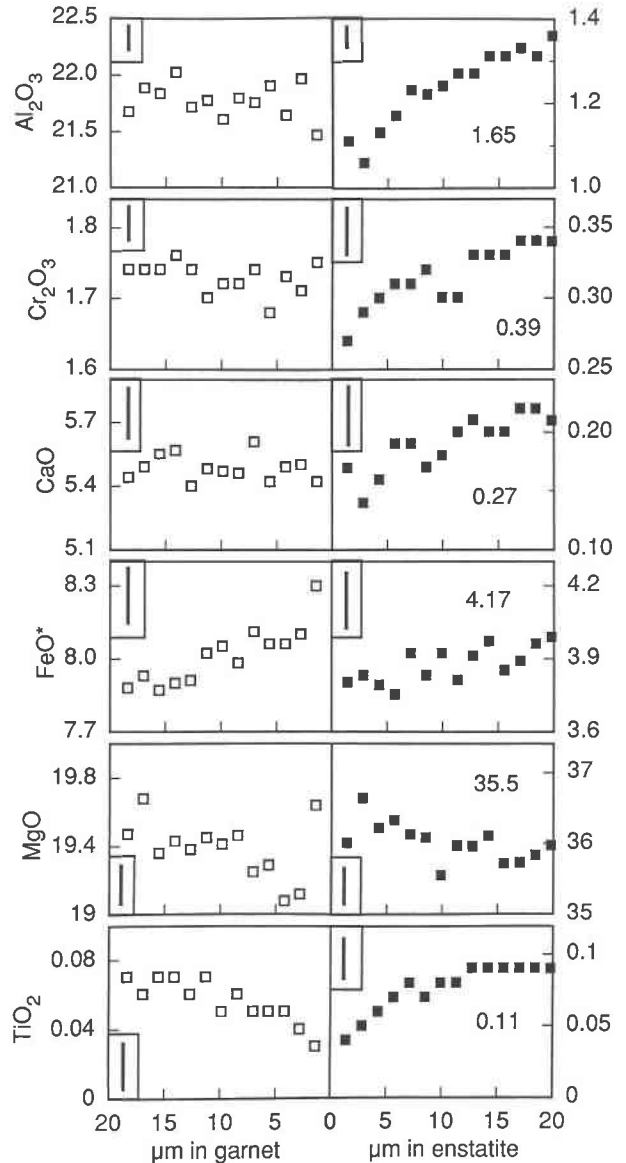

Fig. 7. Wt% oxides across a garnet-pyroxene contact of the crystal shown in Figure 1D and on approximately the same line as the longer traverse shown in Figure 6. Also shown is the composition of the center of the enstatite inclusion analyzed during the same session.

Cr zonation of associated pyroxene, but it is possible that a Cr-zoned garnet rim as thick as several tens of micrometers was once present and then destroyed by the alteration ubiquitous in this rock.

Gradients of Al in pyroxene in the two websterites are much steeper than in the African xenoliths and are matched by an inverse zonation of Mg. The Mg-Al coupling is like that in clinopyroxene with exsolved garnet in the eclogite discussed by Sautter and Harte (1988). Fe and Ca are relatively homogeneous within single orthopyroxene domains (Figs. 4 and 5), consistent with the

observation of Sautter and Harte (1988) that gradients of Mg form as a result of an $Al_2Si_{-1}Mg_{-1}$ substitution even when gradients are not present for other divalent cations. Some garnet adjacent to orthopyroxene (Fig. 5) is zoned to slightly Fe-rich, Ca-poor margins, consistent with exchange with orthopyroxene during cooling, so diffusion was not fast enough to homogenize the garnet.

In addition to the effects of temperature and cooling rate, possible effects of delayed nucleation must be considered in evaluating the compositional gradients, particularly in the pyroxenes of Prs90q. Pyroxenes in this rock retain a much larger range of Al contents than in the other rocks; some garnets in it have irregular, skeletal shapes, and others are packed with pyroxene inclusions. Sautter and Harte (1988) and Jagoutz (1988) have also reported large ranges of Al content within pyroxenes of single xenoliths, and Sautter and Harte (1988) observed that Al-rich pyroxene may survive because garnet nucleated with difficulty. Such delayed nucleation is consistent with experimental evidence of large overstepping of a reaction requiring pyrope nucleation (Boyd and England, 1959).

Zonation of the enstatite included in Navajo pyrope contrasts with that in orthopyroxene in the other rocks because Ca and Fe are distinctly zoned in addition to Al, Mg, and Cr. Gradients of all elements but Ti in the Navajo samples are attributed to garnet-pyroxene interaction. The zonation of Ti to low values at the mutual contacts presumably is due to grain-boundary diffusion of the element to the observed rutile grain.

Zonation of the diopside included in the Navajo megacryst has complexities related to interactions between diffusing elements (Fig. 8). Growth of garnet forms a sink for Al and Cr, and grain-boundary rutile absorbs Ti, thus explaining the gradients of these elements. Na is also zoned to a low at the garnet contact, but no Na sink at the contact has been observed. Jagoutz (1988) explained similar Na gradients as a result of open-system behavior, an impossibility for this diopside inclusion. Na must have diffused into the pyroxene interior to higher concentrations, probably because of the NaCr and NaAl coupling required for charge balance. Uphill diffusion of Na and the associated off-diagonal components in the matrix of diffusion coefficients for diopside may have affected the Al and Cr gradients to different extents, and so relative mobilities of Cr and Al in Na-free diopside cannot be inferred by comparison of the gradients in this inclusion.

Temperature dependences of gradients and inferences for *P-T* calculations

Comparisons of gradients and calculated temperatures are important for evaluating garnet-pyroxene thermobarometry. Differences among the gradients in the three groups of rocks are explicable in terms of these calculated temperatures, although the differences also may have been determined by cooling rates, and effects of delayed nucleation of garnet and of pressure may have been important.

Temperatures calculated by the preferred methods for the two African harzburgites are about 800 °C (Table 1),
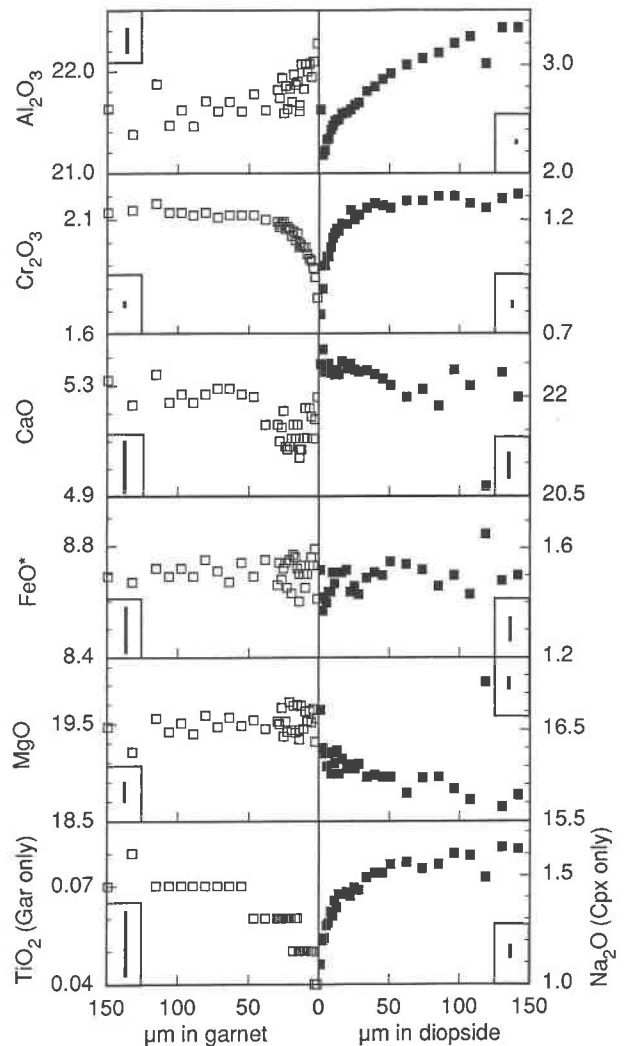

Fig. 8. Wt% oxides across a diopside-pyrope contact (Fig. 1C) in garnet 10, GR1, Garnet Ridge, Arizona. The anomalous compositions in diopside at about 120 μm from the contact are due to an unresolved enstatite lamella.

and the minerals in them are relatively homogeneous. In one rock (J34), the only gradients noted in orthopyroxene were for Cr, and in the other rock (PHN 4803), only slight gradients of Al and Cr were detected in orthopyroxene. Garnet-pyroxene temperatures are lower for the Sullivan Buttes websterites, only ≈600–700 °C, and evidence of disequilibrium is better preserved. The relatively pronounced Al zonation in orthopyroxene may have formed during cooling to these temperatures from about 800 °C, the approximate temperature for the more homogeneous orthopyroxenes. The range of Al_2O_3 (0.75–1.1 wt%) in orthopyroxene lamellae within 5 μm of exsolved garnet in websterite Pr35 may be due to disequilibrium at the contacts or to the steepness of the Al gradients and the uncertainties in measurement of distance. Diffusion was effective in homogenizing Ca within individual orthopy-
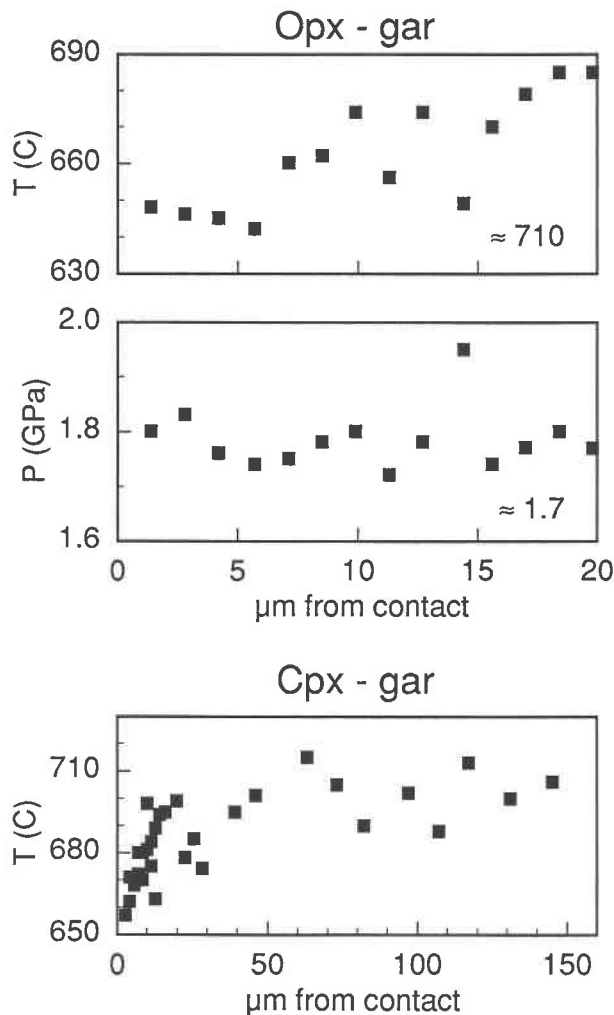
Opx - gar

Fig. 9. Temperatures and pressures calculated with compositions of points equidistant from garnet-pyroxene contacts for two Garnet Ridge, Arizona, samples; values calculated for points removed from the contacts are presented only for comparison with the more meaningful values for compositions near contacts. Orthopyroxene and garnet compositions are in Figure 7; T and P based on the composition of enstatite near the center of the inclusion are also shown. Clinopyroxene and garnet compositions are in Figure 8.

roxene lamellae in this rock, but there are clear differences in CaO (range, 0.12–0.22 wt%) between lamellae, and so Ca apparently did not equilibrate at garnet-orthopyroxene contacts. Similarly, Sautter and Harte (1988) described evidence for lack of equilibration of Ca between clinopyroxene and garnet in exsolution intergrowths.

The preferred pyroxene-garnet temperatures calculated for the Navajo megacrysts are about 650 °C, similar to those for the Sullivan Buttes websterites. Ca gradients in the enstatite inclusion (Fig. 6), however, are far more pronounced than in the websterites (Figs. 3, 4, and 5). These Ca gradients may have been formed as the pyrope me-

gacrysts cooled below the recorded garnet-pyroxene temperatures into the 500–600 °C range calculated from garnet-olivine pairs (Table 1).

Judging from the xenoliths studied here and the preferred geothermometers, equilibrium Al contents in orthopyroxene can be maintained over hundreds of micrometers above ≈800 °C during slow mantle cooling, and Ca and Fe diffusion can be effective to temperatures below 700 °C. Cr diffusion may be slower than that of Al. If the interpretation of a freezing temperature of 1000 °C (Sautter and Harte, 1988, 1990) for a mantle eclogite is correct, then diffusion rates may have been much slower in that environment. Alternatively, the xenolith studied by Sautter and Harte (1988) may have had a different thermal history from the ones studied here; the cooling rate may have been relatively fast if the eclogite was from a small dike emplaced into much cooler mantle, or the cooling could have been from a thermal event just before eruption of the host kimberlite, as noted by Sautter and Harte (1990).

The calculation of pressures and temperatures for peridotite assemblages is often hindered because of alteration at contacts. Gradients measured here can be used to assess P and T calculations based on the interiors of zoned crystals. Gradients such as those in harzburgite PHN 4803 lead to discrepancies only for pressure; use of the 0.98 wt% Al_2O_3 in the interior of an orthopyroxene grain rather than the 0.86 wt% adjacent to garnet leads to pressure underestimates of 0.1 to 0.3 GPa, depending upon the thermobarometer used. Although pyroxenes in the lower temperature websterites and pyrope megacrysts are zoned in Fe and Mg as well as Al, temperatures calculated from compositions of crystal interiors are only 50–70 °C higher than those from within 5 μm of the contacts; calculated pressures do not vary systematically with distance from the contact, because of compensating effects in the Harley (1984a, 1984b) P-T formulation (Fig. 9). Thus even though compositions removed from pyroxene-garnet contacts do not represent equilibrium pairs in these zoned crystals, derived P and T values are approximate guides to those calculated from compositions measured as close to contacts as permitted by resolution of the electron probe. It is possible, however, that none of these calculated P-T pairs represents ambient conditions before eruption of the low-T Arizona samples. Because Al gradients appear to freeze at higher temperature than those of Ca and Fe, the temperatures used in pressure calculation may not be appropriate even if the temperatures calculated from near-contact compositions represented ambient conditions.

Relative gradients at pyroxene-garnet contacts

Lasaga (1983) emphasized the importance of relative diffusion rates in determining the gradients formed by exchange reactions at mineral contacts during cooling: the mineral in which diffusion is relatively fast will have more gentle gradients. Wilson and Smith (1984) documented this difference in a study of olivine included in these py-

rope megacrysts from the Navajo field; they found halos of Fe-enriched garnet about homogeneous olivine inclusions. The reactions discussed here are more complex because of the growth of garnet during cooling, but the principle that more rapid diffusion will lead to more gentle gradients still applies, as long as movement of the contact is minor compared to the distances over which gradients are preserved.

Gradients of Cr are preserved in garnet in many mantle rocks in which pyroxenes are relatively homogeneous (e.g., Harte et al., 1987; Smith and Boyd, 1989). In African harzburgite PHN 4803, much steeper Cr gradients are preserved in exsolved garnet than in adjacent orthopyroxene, and so diffusion of Cr appears significantly slower in garnet than in orthopyroxene at $T \approx 800$ °C (Table 1).

Comparisons of Ca, Fe, and Mg gradients in garnet-pyroxene pairs do not fit an obvious pattern in these rocks. Ca, Fe, and Mg are zoned in one enstatite, but only Fe and Mg appear zoned in enclosing pyrope (Fig. 7). Zonation of Ca and Fe is better defined in garnet than in adjacent orthopyroxene in a websterite (Fig. 5). Fe and Mg appear homogeneous in garnet, but Mg is zoned in the included diopside (Fig. 8). Because neither garnet nor pyroxene is consistently the more homogeneous in these pairs, mobilities of Ca and Fe may be roughly comparable in these minerals at 600–800 °C. Comparisons of the mobility of Mg are complicated by the $Al_2Si_{-1}Mg_{-1}$ substitution in pyroxene (Sautter and Harte, 1988). In addition, diffusion rates in orthopyroxene may be significantly different from those in clinopyroxene, but data here are insufficient to evaluate the possibility.

Simulations of Al gradients in enstatite

The measured gradients and calculated temperatures may be used to calculate limits for effective binary diffusion coefficients. Al in orthopyroxene has been chosen as an example because of its importance in thermobarometry. Gradients of Al_2O_3 in orthopyroxene (Figs. 6 and 7) have been compared to diffusion profiles simulated by a numerical model (Fig. 10, Table 2[1]). The numerical model simulates the diffusion of Al in orthopyroxene in response to changes in concentration at the crystal rim, using a Crank-Nicholson finite-difference approximation modified from a program developed by Barron (1985). Her program itself was a modification of code described by Smith and Wilson (1985) and Wilson and Smith (1984), although these earlier versions utilized a backward time difference rather than a Crank-Nicholson approximation. Press et al. (1989) are among the many who discuss such numerical approaches. Sanford (1982) has described and listed a sophisticated finite-difference program intended for diffusion problems in mineralogy.

[1] Table 2, a listing of the program together with electron probe analyses along traverse paths, can be ordered as Document AM-91-477 from the Business Office, Mineralogical Society of America, 1130 Seventeenth Street NW, Suite 330, Washington, DC 20036, U.S.A. Please remit $5.00 in advance for the microfiche.
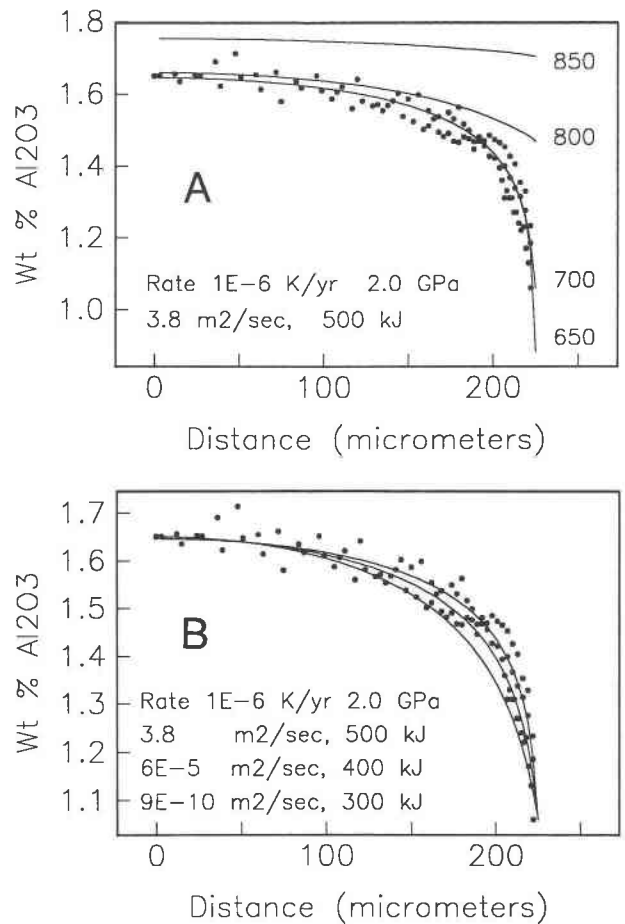

Fig. 10. Results of numerical simulations of Al diffusion in an enstatite inclusion, together with wt% Al_2O_3 plotted as a function of radius. The wt% Al_2O_3 values combine the data of Figures 5 and 6. (A) Simulations of cooling from 1100 °C to 850, 800, 700, and 650 °C at a rate of 10^{-6} degrees/yr and a pressure of 2 GPa. Note the near coincidence of curves for finishing temperatures of 700 and 650 °C. (B) Simulations of cooling from 1100 to 700 °C at a rate of 10^{-6} degrees/yr and a pressure of 2 GPa and from three sets of D_0 (m²/s) and E (kJ).

The ovoid shape of the inclusion (Fig. 1D) was approximated by a sphere. Diffusion coefficients, D, were assumed to fit the formulation, $D = D_0 \, e^{-E/RT}$, with D_0 and E independent of temperature, T. Cooling simulations were begun at 1100 °C with homogeneous enstatite in equilibrium with garnet, and Al_2O_3 concentrations appropriate for that equilibrium were fixed at the orthopyroxene rim at each cooling step. The equilibrium Al_2O_3 concentrations were calculated from the garnet-orthopyroxene compositions and the algorithms of Harley (1984b); to apply these concentrations in the program, Al_2O_3 was expressed as polynomial functions of T at selected pressures using routines from Press et al. (1989). Garnet grows at the grain boundary in response to the flux of Al. Although moving boundaries can be accommodated in numerical models (e.g., Sanford, 1982), the
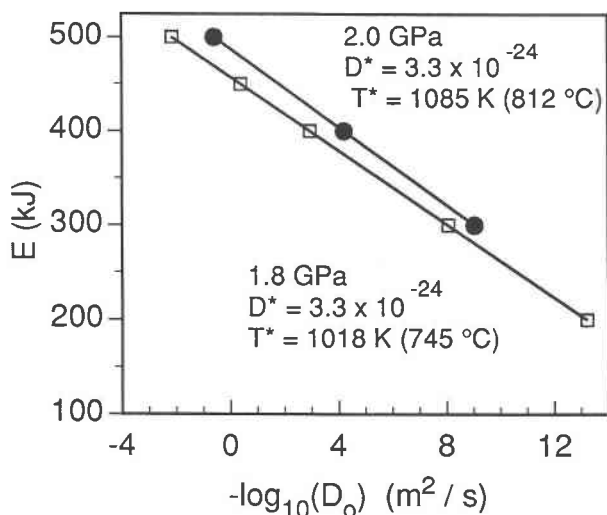
Fig. 11. Plot of E vs. $-\log(D_0)$ for E and D_0 pairs used in numerical simulations yielding good fits to the center and rim compositions of the enstatite inclusion, at 1.8 GPa (squares) and 2.0 GPa (filled circles). D^* and T^* values were derived from the linear arrays.

boundary was assumed fixed in this model because movement is insignificant in comparison to the length of the Al gradients. During cooling from 900 °C at 2 GPa, for instance, a garnet shell about 1.6 μm thick is added at the circumference of the 225-μm radius sphere, based on a mass balance for Al.

Selected simulations are compared to data in Figure 10. In the best simulations, Al is nearly homogeneous at temperatures above 800 °C (Fig. 10A), consistent with the homogeneity of Al in orthopyroxene in the two African xenoliths; because of the homogeneity at higher temperatures in these cooling simulations, starting temperatures are not critical. Finishing temperatures are determined by the boundary condition because the orthopyroxene composition at the garnet contact can be fitted only at one temperature at a given pressure (Fig. 10A). Best fits to the center composition at a given cooling rate and pressure are found for combinations of $\ln(D_0)$ and E that have a near-linear relationship (Fig. 11). The relationship, similar in form to that for diffusing species that share a compensation effect (e.g., Hart, 1981), can be expressed as $\ln(D_0) = \ln(D^*) + E/RT^*$, where D^* and T^* are fitting parameters. For instance, for D_0 and E used in the three simulations shown in Figure 10B, $D^* \approx 3.3 \times 10^{-24}$ m²/s and $T^* \approx 1085$ K. Because all combinations of D_0 and E producing good fits do yield $D = D^*$ at $T = T^*$ for any one linear cooling history, D^* and T^* are particularly useful in comparing results of the simulations to other estimates of diffusivities.

Other criteria must be found to estimate either D_0 or E independently because center and rim compositions can be simulated for combinations that satisfy the above relationship. Curvatures of the simulated profiles provide an additional criterion for comparison of simulations with the data. For simulations with $E < 400$ kJ/mol, calcu-

lated gradients have too little curvature to provide good fits (Fig. 10B). No further attempt was made to restrict acceptable values of E or, in consequence, to restrict further acceptable values of D_0.

Limiting values that can be placed on D_0, E, D^*, and T^* depend primarily upon the constraints that can be placed on cooling histories of the megacrysts. The product of time and D ($= D_0\,e^{-E/RT}$) appears in the solution to diffusion problems, and so a change in rate of cooling in the simulations is compensated by corresponding changes in D, D_0, and D^*. Assumptions of cooling rate are necessarily tenuous considering the complex history of the mantle below western North America. For example, Wilson and Smith (1984) calculated temperature histories for three possible tectonic models, two of which are inconsistent with more recent studies of Colorado Plateau xenoliths (Roden et al., 1990). The lithospheric mantle below the Colorado Plateau probably formed at 1.65–1.9 Ga (Bennett and DePaolo, 1987; Roden et al., 1990). To calculate a minimum rate, cooling in the critical interval from 900 to 600 °C is assumed to have occurred in 1.5 b.y., yielding an average rate of 2×10^{-7} K/yr. Maximum cooling rates are more difficult to assess. Rates of 10^{-6} to 10^{-4} K/yr are plausible for mantle rocks in this critical temperature range, and rates could be much faster.

The fit parameters also depend upon the pressure assumed for equilibration. Gradients of Al_2O_3 become fixed during cooling, as illustrated by the near coincidence of the 700 and 650 °C simulations at 2 GPa (Fig. 10A). If the Al_2O_3 gradients in enstatite were frozen at higher temperatures than Fe and Mg, then the calculated pressure of 1.8 GPa is too low. Because Al diffusion appears to have been slower than that of Fe, judging from a comparison of gradients in other samples, a pressure greater than 1.8 GPa is probably appropriate. At simulated pressures much above 2.0 GPa, however, Al_2O_3 gradients are pronounced above 800 °C even at the low cooling rate of 2×10^{-7} K/yr. Because Al in the harzburgite orthopyroxenes was nearly homogenized by diffusion at about 800 °C, simulations that resulted in pronounced Al zonation much above 800 °C were not utilized. Such simulations would yield smaller diffusivities for Al at a given temperature.

E, D_0, D^*, and T^* values have been calculated for both 1.8 and 2.0 GPa. At the minimum cooling rate of 2×10^{-7} K/yr, D^* and T^* are 6×10^{-25} m²/s and 745 °C in the simulations at 1.8 GPa. At 2.0 GPa, corresponding values are 6×10^{-25} m²/s and 812 °C. Because this cooling rate is a likely minimum, these values of D^* are also likely minimums.

Comparisons

The combined evidence from textures, calculated garnet-pyroxene temperatures of 600–800 °C (Table 1), and measured gradients documents that all cations but Cr diffuse in orthopyroxenes at geologically significant rates to temperatures below $\approx$800 °C in some mantle environments. As disequilibria are frozen in these environments, compositional gradients are preserved in pyroxene on

scales readily measured by electron probe analysis. Gradients of the trivalent cations, Al and Cr, are preserved in orthopyroxene at higher temperatures than those of Ca and Fe. Sneeringer et al. (1984) stated that pyroxenes in the mantle might be out of equilibrium at <1000 °C, however, based on experimental determinations of diffusivities at higher temperatures. The documentation that equilibration took place by diffusion to lower temperatures provides an opportunity to compare estimates of limiting rates of diffusion from natural assemblages with values determined experimentally.

Minimum values for the effective binary diffusion coefficients for Al in orthopyroxene, as estimated from the diffusion simulations, are $D^* = 6 \times 10^{-25}$ m²/s, $T^* = 745$ °C (1.8 GPa simulation) and $D^* = 6 \times 10^{-25}$ m²/s, $T^* = 812$ °C (2.0 GPa simulation). To compare these values with those determined in experiments, extrapolation to higher temperatures is necessary even though highly uncertain. Comparisons are further hindered by the fact that experimental determinations are for clinopyroxene, and diffusivities may be significantly different in orthopyroxene. If a constant activation energy of 400 kJ/mol is assumed, values extrapolated to 1200 °C are $\approx 10^{-18}$ and 8×10^{-20} m²/s for the 1.8 and 2.0 GPa simulations, respectively. These extrapolated values for Al in orthopyroxene are similar to the diffusion rates for Sr and Sm in synthetic diopside determined at 1200 °C by Sneeringer et al. (1984) and greater than the 3×10^{-21} m²/s for Al in diopside at 1180 °C reported by Sautter et al. (1988a). If cooling was faster than the minimum rate of 2×10^{-7} K/yr used in the simulations, then D^* would be greater; for cooling at 10^{-4} K/y and assuming the same 400 kJ activation energy, D^* extrapolates to values of 8×10^{-16} and 4×10^{-17} m²/s at 1200 °C (1.8 and 2.0 GPa simulations), nearer the value of 6×10^{-16} m²/s reported for Al in diopside at 1240 °C by Seitz (1973).

Because neither mineral is consistently more homogeneous in Ca and Fe, mobilities of these elements appear to have been roughly comparable in garnet-pyroxene pairs between 600 and 800 °C. Comparable mobilities also are consistent with the suggestion of Ganguly and Chakraborty (1990) that Fe-Mg interdiffusion parallel to the c axis of orthopyroxene is similar to the diffusion rate in iron manganese garnet in some crustal metamorphic rocks. Much slower diffusion in pyroxene than garnet, however, could be inferred from some experiments. For instance, Brady and McCallister (1983) determined an effective binary interdiffusion coefficient for Ca-Mg in a natural diopside to be about 7×10^{-20} m²/s at 1200 °C, similar to the value of $\approx 2 \times 10^{-20}$ m²/s measured for Mg in pyrope at 800 °C (Cygan and Lasaga, 1985).

Diffusion rates measured in pyroxene at high temperatures cannot be extrapolated to low-T natural environments with confidence, in part because the experimental results span wide ranges (Huebner and Nord, 1981; Sneeringer et al., 1984). In addition, the extrapolations may be misleading because pressure and the f_{O_2}, f_{OH}, and f_H may have large effects on diffusion rates (Goldsmith, 1990; Graham and Elphick, 1990). For example, one xe-

nolith studied here (J34) is from Jagersfontein kimberlite, and Winterburn et al. (1990) noted that the high degree of equilibration in the Jagersfontein suite might have been promoted by the presence of H_2O. The poorly constrained values estimated here from natural environments are useful only because our knowledge of diffusion rates in pyroxenes in the mantle at temperatures near 800 °C is so limited.

REFERENCES CITED

Aines, R.D., and Rossman, G.R. (1984) Water content of mantle garnets. Geology, 12, 720–723.

Anovitz, L.M. (1989) Al-zoning in pyroxenes: Window on prograde granulite P/T paths. Geological Society of America Abstracts with Programs, 21, A183.

Arculus, R.J., and Smith, D. (1979) Eclogite, pyroxenite, and amphibolite inclusions in the Sullivan Buttes Latite, Chino Valley, Yavapai County, Arizona. In F.R. Boyd and H.O.A. Meyer, Eds., The mantle sample: Inclusions in kimberlites and other volcanics, p. 309–317. American Geophysical Union, Washington, DC.

Arculus, R.J., Ferguson, J., Chappell, B.W., Smith, D., McCulloch, M.T., Jackson, I., Hensel, H.D., Taylor, S.R., Knutson, J., and Gust, D.A. (1988) Eclogites and granulites in the lower continental crust: Examples from eastern Australia and southwestern U.S.A. In D.C. Smith, Ed., Eclogites and eclogite-facies rocks, p. 335–386. Elsevier, New York.

Barron, B.R. (1985) Diffusion rate estimates from pyroxene, Garnet Ridge, Arizona. M.A. thesis, University of Texas, Austin, Texas.

Bennett, V.C., and DePaolo, D.J. (1987) Proterozoic crustal history of the western United States as determined by neodymium isotopic mapping. Geological Society of America Bulletin, 99, 674–685.

Boyd, F.R., and England, J.L. (1959) Pyrope. Carnegie Institution of Washington Year Book, 58, 83–87.

Brady, J.B., and McCallister, R.H. (1983) Diffusion data for clinopyroxenes from homogenization and self-diffusion experiments. American Mineralogist, 68, 95–105.

Brey, G.P., and Kohler, T. (1990) Geothermobarometry in four-phase lherzolites II. New thermobarometers, and practical assessment of existing thermobarometers. Journal of Petrology, 31, 1353–1378.

Carswell, D.A., and Gibb, F.G.F. (1987) Evaluation of mineral thermometers and barometers applicable to garnet lherzolite assemblages. Contributions to Mineralogy and Petrology, 95, 499–511.

Cygan, R.T., and Lasaga, A.C. (1985) Self-diffusion of magnesium in garnet at 750 to 900 °C. American Journal of Science, 285, 328–350.

Ellis, D.J., and Green, D.H. (1979) An experimental study of the effect of Ca upon garnet-clinopyroxene Fe-Mg exchange equilibria. Contributions to Mineralogy and Petrology, 71, 13–22.

Finnerty, A.A. (1989) Xenolith-derived mantle geotherms: Whither the inflection? Contributions to Mineralogy and Petrology, 102, 367–375.

Finnerty, A.A., and Boyd, F.R. (1987) Thermobarometry for garnet peridotites: Basis for the determination of thermal and compositional structure of the upper mantle. In P.H. Nixon, Ed., Mantle xenoliths, p. 381–402. Wiley, New York.

Fraser, D.G., and Lawless, P.J. (1978) Palaeogeotherms: Implications of disequilibrium in garnet lherzolite xenoliths. Nature, 273, 220–221.

Freer, R., Carpenter, M.A., Long, J.V.P., and Reed, S.J.B. (1982) "Null result" diffusion experiments with diopside: Implications for pyroxene equilibria. Earth and Planetary Science Letters, 58, 285–292.

Frost, B.R., and Chacko, T. (1989) The granulite uncertainty principle:

Limitations on thermobarometry in granulites. Journal of Geology, 97, 435–450.

Ganguly, J., and Chakraborty, S. (1990) Characterization of metamorphism by Fe-Mg exchange reactions and Sm-Nd geochronology involving garnet: Diffusion kinetic analysis. Geological Society of America Abstracts with Programs, 22, A72.

Goldsmith, J.R. (1990) Pressure-enhanced Al/Si diffusion and oxygen isotope exchange. In J. Ganguly, Ed., Diffusion, atomic ordering and mass transport, p. 221–247. Springer-Verlag, New York.

Graham, C.M., and Elphick, S.C. (1990) Some experimental constraints on the role of hydrogen in oxygen and hydrogen diffusion and Al-Si interdiffusion in silicates. In J. Ganguly, Ed., Diffusion, atomic ordering and mass transport, p. 248–285. Springer-Verlag, New York.

Griffin, W.L., Cousens, D.R., Ryan, C.G., Sie, S.H., and Suter, G.F. (1989) Ni in chrome pyrope garnets: A new geothermometer. Contributions to Mineralogy and Petrology, 103, 199–202.

Harley, S.L. (1984a) An experimental study of the partitioning of Fe and Mg between garnet and orthopyroxene. Contributions to Mineralogy and Petrology, 86, 359–373.

——— (1984b) The solubility of alumina in orthopyroxene coexisting with garnet in FeO-MgO-Al$_2$O$_3$-SiO$_2$ and CaO-FeO-MgO-Al$_2$O$_3$-SiO$_2$. Journal of Petrology, 25, 665–696.

Hart, S.R. (1981) Diffusion compensation in natural silicates. Geochimica et Cosmochimica Acta, 45, 279–291.

Harte, B., and Freer, R. (1982) Diffusion data and their bearing on the interpretation of mantle nodules and the evolution of the mantle lithosphere. Terra Cognita, 2, 273–275.

Harte, B., and Gurney, J.J. (1982) Compositional and textural features of peridotite nodules from the Jagersfontein kimberlite pipe, South Africa. Terra Cognita, 2, 256–257.

Harte, B., Winterburn, P.A., and Gurney, J.J. (1987) Metasomatic and enrichment phenomena in garnet peridotite facies mantle xenoliths from the Matsoku kimberlite pipe, Lesotho. In M.A. Menzies and C.J. Hawkesworth, Eds., Mantle metasomatism, p. 145–220. Academic Press, London.

Hofmann, A.W., and Hart, S.R. (1978) An assessment of local and regional isotopic equilibrium in the mantle. Earth and Planetary Science Letters, 38, 44–62.

Hops, J.J., Gurney, J.J., Harte, B., and Winterburn, P. (1989) Megacrysts and high temperature nodules from the Jagersfontein kimberlite pipe. Geological Society of Australia Special Publication, 14, 759–770.

Huebner, J.S., and Nord, G.L. (1981) Assessment of diffusion in pyroxenes: What we do and do not know. Lunar and Planetary Science, 12, 479–481.

Huebner, J.S., and Voigt, D.E. (1988) Electrical conductivity of diopside: Evidence for oxygen vacancies. American Mineralogist, 73, 1235–1254.

Hunter, W.C., and Smith, D. (1981) Garnet peridotite from Colorado Plateau ultramafic diatremes: Hydrates, carbonate, and comparative geothermometry. Contributions to Mineralogy and Petrology, 76, 312–320.

Jagoutz, E. (1988) Nd and Sr systematics in an eclogite xenolith from Tanzania: Evidence for frozen mineral equilibria in the continental lithosphere. Geochimica et Cosmochimica Acta, 52, 1285–1293.

Krogh, E.J. (1988) The garnet-clinopyroxene Fe-Mg geothermometer—a reinterpretation of existing experimental data. Contributions to Mineralogy and Petrology, 99, 44–48.

Lasaga, A.C. (1983) Geospeedometry: An extension of geothermometry. In S.K. Saxena, Ed., Kinetics and equilibrium in mineral reactions, p. 81–114. Springer-Verlag, New York.

Lee, H.Y., and Ganguly, J. (1988) Equilibrium compositions of coexisting garnet and orthopyroxene: Experimental determinations in the system FeO-MgO-Al$_2$O$_3$-SiO$_2$, and applications. Journal of Petrology, 29, 93–113.

Luth, R.W., Virgo, D., Boyd, F.R., and Wood, B.J. (1990) Ferric iron in mantle-derived garnets: Implications for thermobarometry and for the oxidation state of the mantle. Contributions to Mineralogy and Petrology, 104, 56–72.

McGetchin, T.R., and Silver, L.T. (1970) Compositional relations in minerals from kimberlite and related rocks in the Moses Rock dike, San Juan County, Utah. American Mineralogist, 55, 1738–1771.

O'Neill, H.St.C., and Wood, B.J. (1979) An experimental study of Fe-Mg partitioning between garnet and olivine and its calibration as a geothermometer. Contributions to Mineralogy and Petrology, 70, 59–70.

Pattison, D.R.M., and Newton, R.C. (1989) Reversed experimental calibration of the garnet-clinopyroxene Fe-Mg exchange thermometer. Contributions to Mineralogy and Petrology, 101, 87–103.

Press, W.H., Flannery, B.P., Teukolsky, S.A., and Vetterling, W.T. (1989) Numerical recipes: The art of scientific computing, 818 p. Cambridge University Press, Cambridge, United Kingdom.

Roden, M.F. (1981) Origin of coexisting minette and ultramafic breccia, Navajo volcanic field. Contributions to Mineralogy and Petrology, 77, 195–206.

Roden, M.F., Smith, D., and Murthy, V.R. (1990) Chemical constraints on lithosphere composition and evolution beneath the Colorado Plateau. Journal of Geophysical Research, 95, 2811–2831.

Sanford, R.F. (1982) Three FORTRAN programs for finite-difference solutions to binary diffusion in one and two phases with composition- and time-dependent diffusion coefficients. Computers & Geosciences, 8, 235–263.

Sautter, V., and Harte, B. (1988) Diffusion gradients in an eclogite xenolith from the Roberts Victor kimberlite pipe: 1. Mechanism and evolution of garnet exsolution in Al$_2$O$_3$-rich clinopyroxene. Journal of Petrology, 29, 1325–1352.

——— (1990) Diffusion gradients in an eclogite xenolith from the Roberts Victor kimberlite pipe: (2) Kinetics and implications for petrogenesis. Contributions to Mineralogy and Petrology, 105, 637–649.

Sautter, V., Jaoul, O., and Abel, F. (1988a) Aluminum diffusion in diopside using the ^{27}Al(p,gamma)^{28}Si nuclear reaction: Preliminary results. Earth and Planetary Science Letters, 89, 109–114.

——— (1988b) Aluminum diffusion in diopside. Chemical Geology, 70, 186.

Schulze, D.J., and Helmstaedt, H. (1979) Garnet pyroxenite and eclogite xenoliths from the Sullivan Buttes latite, Chino Valley, Arizona. In F.R. Boyd and H.O.A. Meyer, Eds., The mantle sample: Inclusions in kimberlites and other volcanics, p. 318–329. American Geophysical Union, Washington, DC.

Seitz, M.G. (1973) Uranium and thorium diffusion in diopside and fluorapatite. Carnegie Institution of Washington Year Book, 72, 586–588.

Skogby, H., and Rossman, G.R. (1989) OH$^-$ in pyroxene: An experimental study of incorporation mechanisms and stability. American Mineralogist, 74, 1059–1069.

Skogby, H., Bell, D.R., and Rossman, G.R. (1990) Hydroxide in pyroxene: Variations in the natural environment. American Mineralogist, 75, 764–774.

Smith, D. (1987) Genesis of carbonate in pyrope from ultramafic diatremes on the Colorado Plateau, southwestern United States. Contributions to Mineralogy and Petrology, 97, 389–396.

Smith, D., and Boyd, F.R. (1989) Compositional heterogeneities in minerals of sheared lherzolite inclusions from African kimberlites. Geological Society of Australia Special Publication, 14, 709–724.

Smith, D., and Wilson, C.R. (1985) Garnet-olivine equilibration during cooling in the mantle. American Mineralogist, 70, 30–39.

Sneeringer, M., Hart, S.R., and Shimizu, N. (1984) Strontium and samarium diffusion in diopside. Geochimica et Cosmochimica Acta, 48, 1589–1608.

Stosch, H.-G., Lugmair, G.W., and Kovalenko, V.I. (1986) Spinel peridotite xenoliths from the Tariat Depression, Mongolia. II: Geochemistry and Nd and Sr isotopic composition and their implications for the evolution of the subcontinental lithosphere. Geochimica et Cosmochimica Acta, 50, 2601–2614.

Wells, P.R.A. (1977) Pyroxene thermometry in simple and complex systems. Contributions to Mineralogy and Petrology, 62, 129–139.

Wilson, C.R., and Smith, D. (1984) Cooling rate estimates from mineral zonation: Resolving power and applications. In J. Kornprobst, Ed., Kimberlites. II: The mantle and crust-mantle relationships, p. 265–275. Elsevier, Amsterdam.

Winterburn, P.A., Harte, B., and Gurney, J.J. (1990) Peridotite xenoliths from the Jagersfontein kimberlite pipe: I. Primary and primary-metasomatic mineralogy. Geochimica et Cosmochimica Acta, 54, 329–341.

Appendix Table 1. Mineral compositions for *P-T* calculations

	1a	1b	1c	2a	2b	2c	2d	3a	3b	3c	3d
SiO_2	57.3	54.4	42.1	58.3	54.5	42.2	42.3	54.4	42.1	41.6	41.8
TiO_2	n.d.	n.d.	n.d.	n.d.	0.02	n.d.	n.d.	0.16	0.04	n.d.	0.08
Al_2O_3	0.86	2.32	21.7	0.75	2.36	21.4	n.d.	2.06	22.1	n.d.	22.2
Cr_2O_3	0.28	1.44	2.56	0.22	1.73	2.65	n.d.	0.93	1.85	n.d.	1.99
FeO^*	4.86	1.69	8.25	4.73	1.84	8.17	7.70	1.38	8.79	6.29	8.59
MgO	36.0	16.4	20.2	35.8	15.8	20.1	51.7	16.4	19.3	51.4	19.3
CaO	0.23	21.3	4.99	0.22	21.3	4.90	0.02	22.6	5.18	0.02	5.49
Na_2O	0.05	1.54	n.d.	0.04	1.77	n.d.	n.d.	1.19	0.02	n.d.	n.d.
Sum	99.6	99.1	99.8	100.1	99.3	99.4	101.7	99.1	99.4	99.3	99.5

	4a	4b	4c	4d	5a	5b	5c	6a	6b	6c
SiO_2	58.0	42.2	41.5	42.3	56.7	54.9	40.2	56.9	54.1	41.2
TiO_2	0.05	0.04	n.d.	0.09	0.02	0.14	0.02	n.d.	0.23	0.02
Al_2O_3	1.06	22.0	n.d.	22.8	0.75	3.71	22.7	1.10	5.28	23.0
Cr_2O_3	0.29	1.71	n.d.	1.73	0.06	0.32	0.41	0.16	0.88	0.70
FeO^*	3.83	8.10	5.62	7.86	14.0	4.47	21.9	9.08	2.57	16.1
MgO	36.6	19.1	52.4	20.4	30.0	14.1	10.7	33.2	14.0	14.5
CaO	0.14	5.50	n.d.	5.25	0.11	20.9	5.08	0.14	21.2	5.10
Na_2O	n.d.	n.d.	n.d.	0.02	n.d.	2.24	n.d.	n.d.	1.77	0.02
Sum	100.0	98.7	99.5	100.6	101.6	100.8	101.0	100.6	100.1	100.7

Note: n.d. is not detected. Samples as follows: (1) PHN 4803: a, opx; b, cpx; c, garnet. (2) J34: a, opx; b, cpx; c, garnet; d, olivine. (3) Garnet 10, GR1: a, cpx and b, garnet, each 2.8 μm from contact; c, olivine and d, nearby garnet. (4) Garnet 1, GR1: a, opx and b, garnet, each 2.8 μm from contact; c, olivine and d, nearby garnet. (5) Pr35: a, opx; b, cpx; c, garnet—all lamellae. (6) Prs90q: a, opx; b, cpx; c, garnet.